Aesth Plast Surg (2019) 43:233–242
https://doi.org/10.1007/s00266-018-1238-3

ISAPS CrossMark

ORIGINAL ARTICLE BASIC SCIENCE/EXPERIMENTAL

Smooth Muscle Alpha Actin Immunoexpression (α-Sma) and CD-117 Antibody (C-Kit) in Capsules Formed by Polyurethane Foam-Coated Silicone Implants and with Textured Surface: A Study on Rats

Eduardo Nascimento Silva[1,2] · Jurandir Marcondes Ribas-Filho[1] · Fernando Issamu Tabushi[1] · Majenna Andrade Pachnicki Silva[3] · Elisa Beatriz Dalledone Siqueira[1] · Lucia de Noronha[4] · Alfredo Benjamim Duarte da Silva[2,5] · Leandro Cavalcante Lipinski[6] · Isabelle Guth[1] · Larissa Maria Vosgerau[1]

Received: 6 July 2018 / Accepted: 9 September 2018 / Published online: 1 October 2018

Abstract

Background One of the undesirable complications that might occur after breast augmentation with silicone implants is capsular contracture. In its etiology, the relations between mast cells and myofibroblasts play an important role in collagen synthesis. Mast cells are able to activate fibroblasts into myofibroblasts, through paracrine secretions, inducing collagen production. The objectives of this study were to analyze the myofibroblast concentration through the α-SMA immunomarker and evaluate the intensity of mast cell expression against the C-Kit immunomarker.

Material and Method Sixty-four Wistar rats were used, divided into two groups (polyurethane foam and textured surface) with 32 animals in each. The animals received silicone implants on the back, below the *panniculus carnosus*, and after the determined period, they were killed and the capsules formed around the implants were studied. The capsules were analyzed employing the immunohistochemical technique, with the α-SMA and C-Kit immunomarkers in subgroups of 30, 50, 70 and 90 days.

Results The myofibroblast concentration was higher in the polyurethane group when compared to the textured group (30 days $p = 0.105$; 50 days $p = 0.247$; 70 days $p = 0.014$ and 90 days $p = 0.536$). The intensity of mast cell expression was more pronounced in the polyurethane group when compared to the textured group (30 days $p = 0.798$; 50 days $p = 0.537$; 70 days $p = 0.094$ and 90 days $p = 0.536$).

Conclusions Polyurethane-coated implants induced higher concentrations of myofibroblasts and higher expression of mast cells, when compared to the textured surface implants.

No Level Assigned This journal requires that authors assign a level of evidence to each article. For a full description of these Evidence-Based Medicine ratings, please refer to the Table of Contents or the online Instructions to Authors www.springer.com/00266.

Keywords Implant capsular contracture · Breast implants · Mammaplasty · Immunohistochemistry

Research performed at Postgraduate Program in Principles of Surgery, Faculdade Evangélica do Paraná (FEPAR), Evangelic University Hospital (HUEC) and Institute for Medical Research (IPEM), Curitiba-PR, Brazil.

Electronic supplementary material The online version of this article (https://doi.org/10.1007/s00266-018-1238-3) contains supplementary material, which is available to authorized users.

✉ Eduardo Nascimento Silva
dr_eduardosilva@yahoo.com.br

[1] Evangelical Faculty of Medicine of Paraná (FEPAR), Evangelical University Hospital of Curitiba (HUEC) and Institute for Medical Research (IPEM), Curitiba, PR, Brazil

[2] Plastic Surgery and Anatomy, State University of Ponta Grossa (UEPG), Avenida Doutor Francisco Búrzio, 991, 84010-200 Ponta Grossa, PR, Brazil

[3] Ponta Grossa, PR, Brazil

[4] Anatomical Pathology, Pontifical Catholic University of Paraná (PUC-PR), Curitiba, PR, Brazil

[5] Operative Technique, Federal University of Paraná (UFPR), Curitiba, PR, Brazil

[6] Operative Technique, State University of Ponta Grossa (UEPG), Ponta Grossa, PR, Brazil

Introduction

The most performed plastic surgery worldwide is breast augmentation [1]. All material introduced into the human body provokes a foreign body reaction with formation of a fibrous capsule around it [2, 3]. The capsule might become hard, causing deformity and breast pain, a condition known as capsular contracture [4–6].

Regarding its etiopathogenesis, many studies have already been carried out researching the variety of factors involved: implant coating, biofilm formation, hematoma, unsuitable surgical technique, pathological healing, among others [3, 7–17].

Nowadays, the most used types of coating in silicone implants are smooth, textured (nano, micro, intermediate and macro) and polyurethane foam [1, 18–21]. From these, the one with the lowest capsular contracture rate in breast augmentation is polyurethane foam with a 0.4–1% rate, followed by textured implants with 2–15% [19].

One of the reasons is the fact that polyurethane foam biodegradation, through hydrolysis, prevents the adhesion of fibroblasts and endothelial cells to the capsule collagenous layer, reducing the risk of contracture and extending the inflammatory reaction [12, 22].

Also, during this process, new resulting vectors are created on the surface of the silicone implant, with different lengths and directions, which justify the lower incidence of capsular contracture in this type of coating [23].

Polyurethane-coated implants, in spite of developing thicker capsules, show an increase in non-collagenous capsules, and, therefore, present lower amounts of type I collagen, when compared to textured implants [15, 22, 24, 25].

One unfavorable characteristic of the macro-textured implants and those with polyurethane foam is that they present a higher surface area, which makes them more prone to biofilm formation. In their surface grooves, the bacteria find a larger area to fix themselves. This is relevant, because the risk of developing large cell anaplastic carcinoma is 14.11 times higher with Biocell® (Allergan, Dublin, Irlanda) implants and 10.84 times higher with polyurethane implants [26].

As regards capsular contracture, the last publications on the theme emphasize the cell interrelations and their relations with inflammatory mediators. In the cell environment, studies have been developed on the factors that lead fibroblasts to transform into myofibroblasts with a smooth muscle alpha actin positive marker (α-SMA), and also how this transformation is mediated by macrophages, T cells and mast cells [3, 13, 16, 27–33].

Recently, the presence of toll-like receptor 4 in fibroblasts and myofibroblasts has been reported and correlated positively with estrogen receptors beta. These receptors, when activated, induce a pro-fibrotic state with the transformation of fibroblasts into myofibroblasts, and this process is closely related to the female hormone estradiol [16].

Receptors (AT_1R, H_1R and TGF-βRI) were also identified in fibroblasts, with expression for mediators produced by mast cells (renin, histamine and the transform growth factor beta). Another important connection between mast cells and fibroblasts is the intercellular junctional communications, which present six connexin proteins in their constitution, among which connexin 42 outstands. Thus, through paracrine secretions, mast cells are able to induce collagen production, activating fibroblasts and myofibroblasts [27, 28, 30, 33–35].

After activated, myofibroblasts become an important collagen producing source, and this might contribute to the development of capsular contracture [13, 16, 29, 32, 33, 36, 37]. In hypertrophic scars, there is a predominance of mast cells, which in a normal scar do not appear in great number [29, 35].

The objective of this study was to compare the intensity of the expression of mast cells, the myofibroblast concentrations, and to compare the capsules formed by polyurethane-coated silicone implants and those with a textured surface.

Materials and Methods

This study was carried out at the vivarium of a State University, after being approved by the Animal research ethics Committee. All experimental steps were assisted by the presence of a veterinarian.

The study comprises a double-blind randomized clinical test, in which 64 Wistar rats (*Rattus norvegicus*) weighing between 190 and 250 g, aged between 30 and 90 days, were used. The animals were distributed in 500 cm^3 acrylic boxes with four animals in each. They received free access to water and feed appropriate to the species, at room temperature and 12 h circadian cycles. They were divided into two groups with 32 animals each and called the polyurethane group and textured group. They were then subdivided into four subgroups according to the time when death occurred (30, 50, 70 and 90 days).

The silicone implants used were polyurethane foam-coated and textured surface, both donated by the company Silimed (Maximum®, Rio de Janeiro, Brazil).

Experimental Steps

The rats were anesthetized using intraperitoneal injection of 1% ketamine (40 mg/kg) and 2% xylazine (8 mg/kg).

Next, they were put in the prone position and trichotomy was performed on the back. The surgical procedure was carried out in antiseptic conditions and with sterilized silicone implants and surgical material.

The incision was performed on the back and the pocket that housed the implants was made on the retromuscular plane with scissors in a cranial direction, starting 5 mm from the incision and with a square shape. The implants were inserted and placed 5 mm from the incision. The skin suture was performed with three simple stitches using mononylon 5-0 (Fig. 1 and Video 1) (Mononylon Ethilon®, Ethicon Incorporation, New Jersey, USA).

The wound was kept exposed, and postoperative analgesia was applied with a single, intramuscular injection of dipyrone (20 mg/kg) on the outside of the hind limb [15, 38]. There were no postoperative dressings or stitch removal.

The rats were killed according to their subgroups with an application of ketamine and xylazine, corresponding to four times the therapeutic dose and subsequent cervical dislocation. Seven animals were excluded due to implant extrusion—four from the polyurethane group (2 from the 50-day, 2 from the 70-day and 1 from the 90-day subgroup) and three from the textured group (all of them from the 50-day subgroup).

The histological material was obtained upon bloc resection, from the skin to the muscular plane, with the surgical margins of the anatomical pieces 5 mm from the edge of the discoid implants (Fig. 2 and Video 2).

Immunohistochemical Evaluation

The tissue microarray technique (TMA) was employed in this research, which consists of a paraffin block holding several samples of different tissues, whose relevant areas for immunohistochemical stain were collected from several donor blocks and rearranged on a single receiving block [39, 40].

The immunohistochemical method was used with the indirect technique employing the smooth muscle alpha acting markers (α-SMA, 1:400, Dako, clone 1A4) and CD-117 antibody (C-Kit, 1:100, Dako, clone A4502). The pathologist did not know which animal group was being investigated. During the result analysis, they selected the best slides for photomicrographic documentation.

The immunomarked slides were then read, using an optical microscope (Axio Scope.A1®, Zeiss, Oberkochen, Germany), coupled to a digital camera (AxioCam MRc®, Zeiss) and a computer with image analysis software (AxioVision®, Zeiss). Images were captured in a 400 × high power field (HPF), whose total area was 144.073,3 μm^2, with a 1024 × 768 pixel resolution, for each case of the study.

A HPF image was chosen for the mask confection, showing the suitable positivity for the biomarker chosen. An image of the rats in the experiment was used rather than one from the reaction control (Fig. 3).

The mask was then overlapped to the digital images of the cases. Based on its ideal immunopositivity, the image analysis software (Image Pro-Plus®, Media Cybernetics,

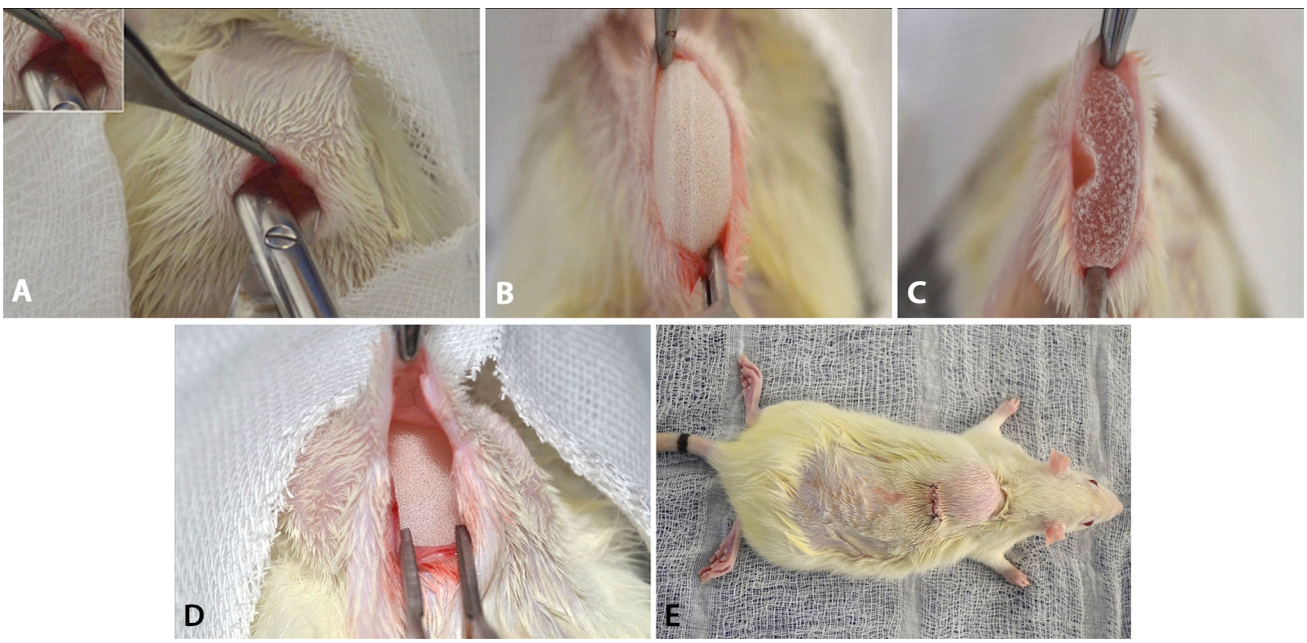

Fig. 1 **a** Pocked creation in the *panniculus carnosus* to house the implant; **b** introduction of polyurethane-coated implant; **c** introduction of the textured surface implant; **d** implant positioned 5 mm from the incision; **e** final aspect in the immediate postoperative

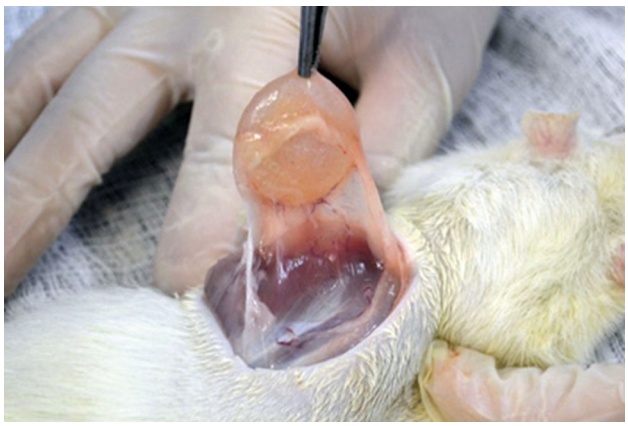

Fig. 2 Bloc resection of the piece for histological study

Rockville, USA) found the immunopositive areas in the samples and transformed this data into immunopositive area per square micrometer (μm^2) (Fig. 4).

The area in μm^2 generated by this method was then divided by the constant 144.073,3 μm^2, which is the total area of the field under evaluation, generating a percentage of immunopositive area through HPF. The mean percentage of area in HPF was calculated for each case.

Statistical Analysis

For the analysis presented below, the percentage of expression of the α-SMA and C-Kit immunomarkers was considered. From the results of the slide reading, data were obtained as: 100 × positive area/(positive area + negative area). This indicates that the variables under analysis (α-SMA and C-Kit) correspond to the 'positive' area mean in relation to the total 'positive' and 'negative' areas. The statistical analysis was assisted by the software IBM SPSS Statistics v.20® (International Business Machines, North Castle, USA).

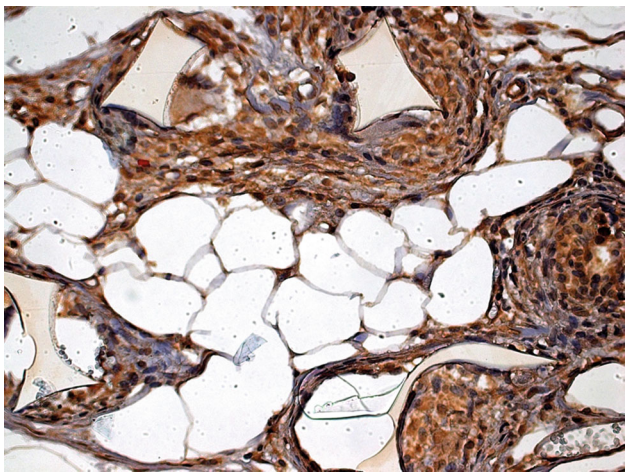

Fig. 3 Photomicrograph showing smooth muscle alpha actin immunomarked myofibroblasts, in the absence of polarized light and myofibroblasts stained in brown (× 400)

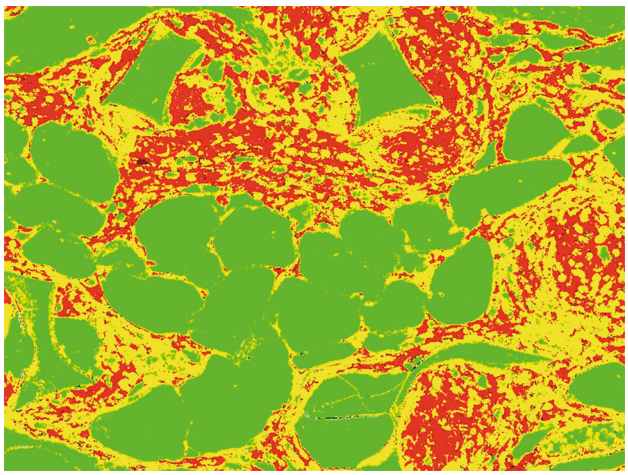

Fig. 4 The same previous photomicrograph after the application of the mask by the software *Image Pro-Plus* in the absence of polarized light and positive expression of the immunomarker in red (× 400)

Results

Immunohistochemical Markers

Smooth Muscle Alpha Actin Marker (α-SMA)

In all groups analyzed (30, 50, 70 and 90 days), the mean of the positive area percentage for the α-SMA immunomarker was higher in the polyurethane group, and in the subgroup 70 days, it was statistically significant (Table 1 and Fig. 5).

Figure 6 illustrates the differences of positive area percentages for the α-SMA immunomarker between each of the groups in the different subgroups under analysis.

Table 2 shows the "*p*" values of the results of α-SMA positivity percentages in each group, comparing all the subgroups, to verify whether a statistical difference would be found between the groups.

CD-117 Antibody Marker (C-Kit)

In all subgroups under analysis (30, 50, 70 and 90 days), the mean of positive area percentage of the C-kit immunomarker was higher in the polyurethane group, however, without statistical significance (Table 3 and Fig. 7).

Figure 8 illustrates the differences of positive area percentages for the C-Kit immunomarker between each group in the different subgroups under analysis.

Table 1 Comparison of the α-SMA percentage in both groups and in each subgroup

Subgroup	Group	α-SMA—positive area percentage						*p** value (*P* × *T*)
		n	Mean	Median	Minimum	Maximum	Standard deviation	
30	P	8	30.7	31.9	20.3	37.8	6.0	
	T	8	20.7	23.6	3.4	34.1	12.7	0.105
50	P	6	21.9	21.0	12.2	35.9	8.1	
	T	5	17.7	10.8	2.4	53.6	20.9	0.247
70	P	7	30.2	26.6	22.2	44.1	8.8	
	T	8	16.5	16.2	5.4	30.7	8.0	**0.014**
90	P	7	31.5	32.1	12.7	48.0	14.1	
	T	8	26.6	16.4	10.9	69.7	22.8	0.536

*Mann–Whitney nonparametric test, $p < 0.05$

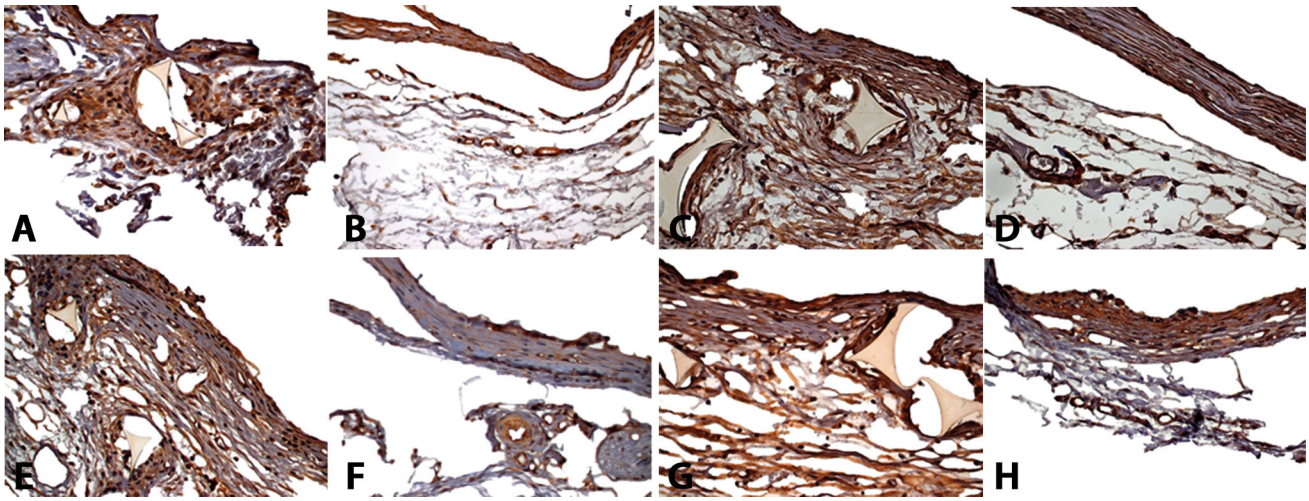

Fig. 5 Photomicrograph of the polyurethane foam-coated silicone implants and those with textured surface showing the myofibroblasts in each group and in the different subgroups in the absence of polarized light and myofibroblasts stained in brown (× 400). **a**, **c**, **e**, **g** Polyurethane; **b**, **d**, **f**, **h** textured surface

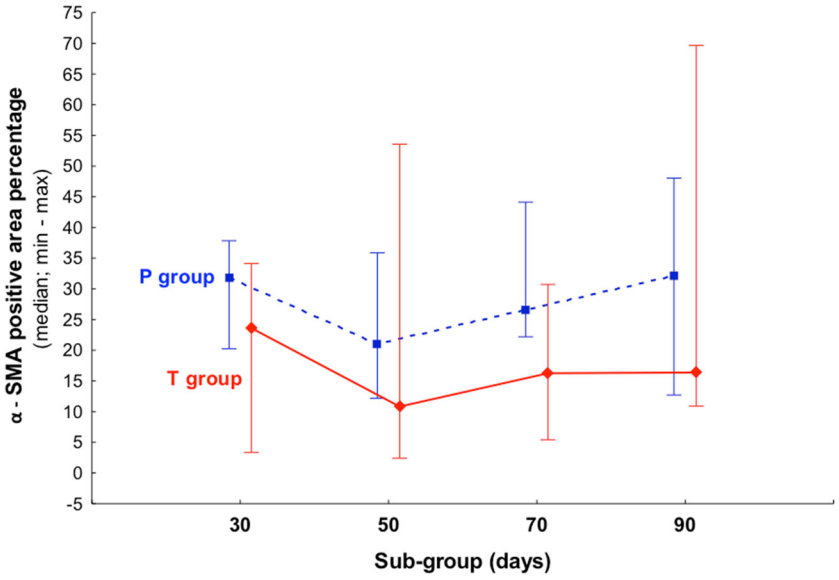

Fig. 6 Percentages of smooth muscle alpha actin between each group in the subgroups under analysis

Table 2 Comparison of α-SMA percentage values in each group between the subgroups

Group	p* value (30 × 50 × 70 × 90)
P	0.249
T	0.690

*Kruskal–Wallis nonparametric test, $p < 0.05$

Table 4 presents "p" values of the results of the C-Kit positivity percentages in each group, comparing all subgroups, to verify whether a statistical difference would be found between the groups.

A significant difference was found in the textured group, between the subgroups 30, 50, 70 and 90 days, in relation to the C-Kit positive area percentage ($p = 0.017$). Thus, the groups were compared in pairs, to see which groups presented statistical significance (Table 5).

As explained above, in the textured group, when the different subgroups were compared one to the other, statistical significance was observed between the subgroups 30 and 70 days ($p = 0.004$) and between the 30 and 90 days ($p = 0{,}003$).

Discussion

The rat (*Rattus novergicus albinus*, Roentia mammalia), chosen by the author, is the most used in capsular contracture studies for presenting easy reproducibility of results, resistance to surgical intervention, high availability in vivarium, and the capsules formed around the silicone

Table 3 Comparison of the C-Kit percentages in both groups and in each subgroup

Subgroup	Group	C-Kit—positive area percentage						p* value ($P \times T$)
		n	Mean	Median	Minimum	Maximum	Standard deviation	
30	*P*	8	19.1	20.4	6.8	31.2	8.7	
	T	8	18.0	17.4	12.5	24.2	4.0	0.798
50	*P*	6	17.7	15.4	9.2	27.1	7.6	
	T	5	13.7	11.1	3.7	31.9	11.5	0.537
70	*P*	7	14.6	13.6	5.5	25.5	6.6	
	T	8	8.8	6.5	4.7	18.5	5.0	0.094
90	*P*	7	10.1	8.1	1.9	18.2	6.4	
	T	8	8.3	7.2	1.7	16.0	4.9	0.536

*Mann–Whitney nonparametric test, $p < 0.05$

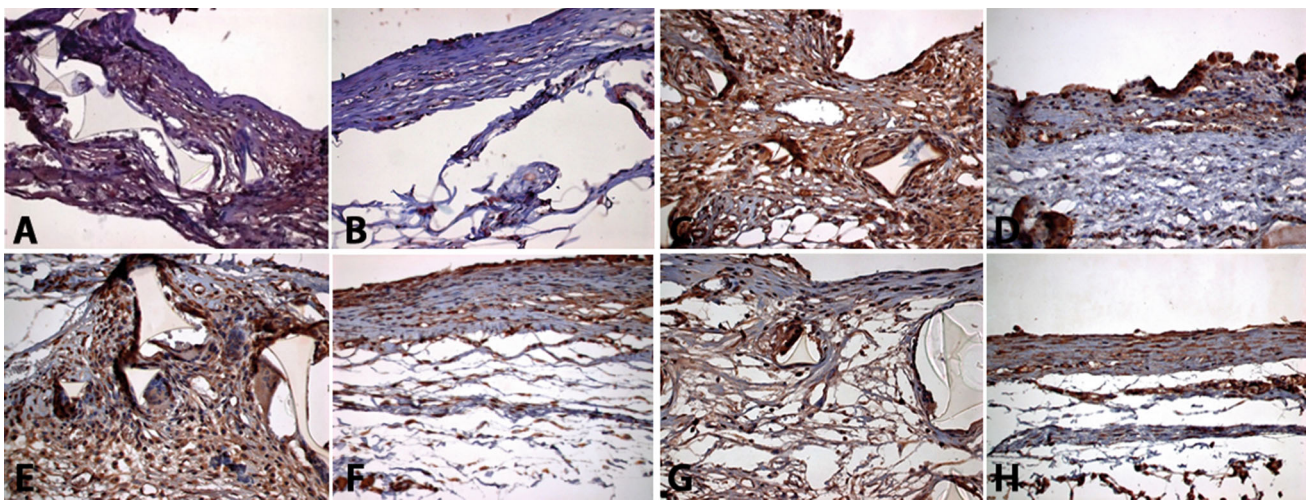

Fig. 7 Photomicrograph of the polyurethane foam-coated silicone implants and those with textured surface, evidencing mast cells in each group and in the different subgroups, in the absence of polarized light and mast cells stained in brown (× 400). **a** **c**, **e**, **g** Polyurethane; **b**, **d**, **f**, **h** textured surface

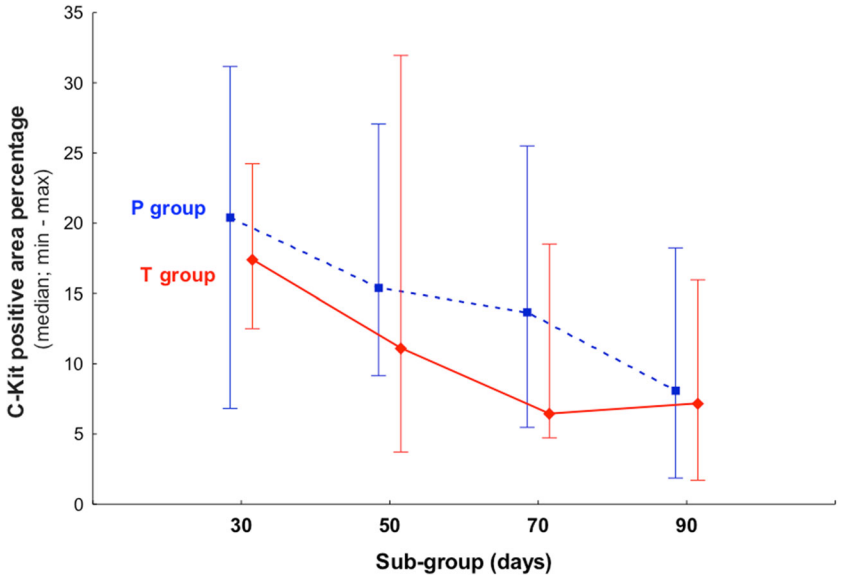

Fig. 8 Positive area percentage for the CD-117 antibody (C-Kit) between each group and in the subgroups under analysis

Table 4 Comparison of C-Kit percentage values in each group and between the subgroups

Group	p* value (30 × 50 × 70 × 90)
P	0.149
T	**0.017**

*Kruskal–Wallis nonparametric test, $p < 0.05$

Table 5 Comparison of the C-Kit positive area percentages in two subgroups within the textured group, evaluating statistical significance

Subgroups compared	p* value
30 × 50	0.060
30 × 70	**0.004**
30 × 90	**0.003**
50 × 70	0.411
50 × 90	0.347
70 × 90	0.891

*Fisher's exact test, $p < 0.008$ (Bonferroni correction)

implants can be studied in these animals after a 30-day period [2, 12, 15, 22, 41–49].

The reason that polyurethane foam-coated implants and those with a textured surface were chosen is that both implants present the lowest rates of capsular contracture, which were 0.4–1% and 2–15%, respectively [19].

A close relation between fibroblasts and mast cells was seen which might lead to the pro-fibrotic condition. From the evidence that supports this fact, we highlight the identification of receivers in fibroblasts (AT_1R, H_1R and TGF-βRl) with expression for the mediators produced by the mast cells (renin, histamine and TGF-β), and the existence of intercellular junctional communications, mainly connexin 43 [35].

Recent studies involving in vitro cell culture have demonstrated that through intercellular junctional communications the mast cells influence the proliferation of fibroblasts, the contraction of the fibroblast populated collagen net, a greater transformation of fibroblasts to myofibroblasts and reduced migration of fibroblasts and that degranulated mast cells present similar behavior, due to the maintenance of these intercellular communications [27, 28].

Regarding the intercellular relation, mast cells were seen to prevent dexamethasone-induced cell death in fibroblasts cultivated in vitro. Junctional communications between the mast cells and fibroblasts prevent the apoptosis of these cells, resulting in a greater number of fibroblasts and myofibroblasts, which might be related to hypertrophic scar genesis [29].

Thus, through paracrine secretions, the mast cells are able to induce collagen production through fibroblasts [30]. The mast cell released chymase results in an increase in the TGF-β1/ SMAD intracellular signaling, resulting in proliferation of fibroblasts in hypertrophic scars and in collagen synthesis [33].

An interesting fact is that a small number of mast cells can activate a great number of fibroblasts into myofibroblasts, in a 1:10 ratio, to obtain maximum collagen synthesis [28], while in situations where inactive mast cells are activated, it results in the normalization of the number of myofibroblasts and collagen [51].

Another way of activating mast cells is through the bacteria *Staphylococcus aureus*. In an in vitro study, they

were incubated with cytochalasin D or with anti-receptor antibodies toll 2 or anti-CD 48, and their cell invasion ability and that of initiating an inflammatory response were inhibited [53].

In a study on capsular contracture in humans, the presence of mast cells around the capsules formed on silicone implants was analyzed, and a greater number of mast cells were found in the posterior capsular portion rather than in the anterior one. Baker IV capsules showed greater numbers of fibroblasts when compared to Baker I capsules [30].

An attempt to reduce collagen production upon the inhibition of mast cells has been the use of off-label anti-leukotrienes. In a study with rats with textured silicone implants which received a 5 mg/kg/day zafirlukast dose, lower numbers of mast cells were found when compared to the control group, which did not receive this medication [43].

The present study is the first in the literature to evaluate the presence of mast cells quantitatively. In both groups, in all subgroups under evaluation, myofibroblasts were evidenced by α-SMA, always concomitantly to mast cells, visualized by the use of the C-Kit immunomarker.

With results slightly different than the ones in this study, Bui et al. [50] reported the absence of positive α-SMA immunoreactivity in all capsules formed around textured implants. However, it seems relevant to emphasize that those authors researched humans, and this research was developed with rats.

In a recent publication, Silva et al. [15] compared histologically the capsules formed by polyurethane foam implants and those with textured surface. They found a result similar to the result of this study, with the polyurethane group, in all subgroups under evaluation, presenting higher numbers of myofibroblasts, when compared to the textured group.

Similarly to Vieira et al. [22], the animals in the polyurethane group showed more pronounced expression of the α-SMA marker in all subgroups under evaluation when compared to the textured group. The difference between the studies is the fact those authors obtained statistical significance in the subgroup 30 days, whereas in this study, the results were statistically significant in the subgroup 70 days.

Unlike Hwang et al. [52], who stated that there was no influence of the implant coating in the number of myofibroblasts, in this study, the polyurethane foam implants presented higher numbers of fibroblasts. However, those authors compared textured and smooth implants, in humans, while in this study, polyurethane and textured surface implants in rats were compared.

The results of this study do not agree with those found by Younan et al. [9], who reported higher collagen maturation upon activation of mast cells through microdeformational wound therapy (vacuum assisted closure); in this study in both groups in all subgroups under evaluation, mast cells were found in an inversely proportional relation with the period of analysis. That is, the later the period under analysis was, the lower the number of mast cells was.

These data are also in agreement with Silva et al. [15], who found in the relation time dependence, higher amounts of mature collagen (type I) and lower amounts of immature collagen (Type III), in groups with polyurethane and textured implants, in all subgroups.

Conclusion

Polyurethane foam-coated silicone implants induced higher concentrations of fibroblasts and a higher intensity of mast cell expression, when compared to textured surface implants. In relation to the area percentage expressed by mast cells, statistical difference was found in the textured group between the different subgroups under analysis, and when the groups were compared one to another, there was statistical significance between 30 and 70 days and 30 and 90 days.

Authors' Contributions Eduardo Nascimento Silva contributed to conception, design, intellectual and scientific content of the study, technical procedures, and statistical analysis. Jurandir Marcondes Ribas-Filho involved in scientific and intellectual content of the study, interpretation of data, critical revision and final approval. Fernando Issamu Tabushi and Alfredo Benjamim Duarte da Silva helped in scientific and intellectual content of the study, interpretation of data and critical revision. Majenna Andrade Pachnicki Silva contributed to acquisition of data, technical procedures and manuscript preparation. Elisa Beatriz Dalledone Siqueira involved in conception, design, intellectual and scientific content of the study. Lucia de Noronha performed interpretation of data and histopathological examinations. Leandro Cavalcante Lipinski helped in scientific content of the study and technical procedures. Isabelle Guth and Larissa Maria Vosgerau contributed to acquisition of data and technical procedures.

Compliance with Ethical Standards

Ethics Committee Approval State University of Ponta Grossa (UEPG).

References

1. Maxwell GP, Gabriel A (2014) The evolution of breast implants. Plast Reconstr Surg 134(1S):12S–17S
2. Mendes PRS, Bins-Ely J, Lima EAS, Vasconcellos ZAA, D'acampora AJ, Neves RE (2008) Histological study on acute inflammatory reaction to polyurethane-coated silicone implants in rats. Acta Cir Bras 23(1):93–101
3. Major MR, Wong VW, Longaker MT, Gurtner GC (2015) The foreign body response: at the interface of surgery and bioengineering. Plast Reconstr Surg 135(5):1489–1498

4. Poeppl N, Schreml S, Lichtenegger F, Lenich A, Eisenmann-Klein M, Prantl L (2007) Does the surface structure of implants have an impact on the formation of a capsular contracture? Aesthet Plast Surg 31(2):133–139
5. Araco A, Caruso R, Araco F, Gravante JOG (2009) Capsular contractures: a systematic review. Plast Reconstr Surg 124(6):1808–1819
6. Moyer KE, Ehrlich HP (2013) Capsular contracture after breast reconstruction: collagen fiber orientation and organization. Plast Reconstr Surg 131(4):680–685
7. Lu F, Gao J, Ogawa R, Hyakusoku H (2007) Variations in gap junctional intercellular communication and connexin expression in fibroblasts derived from keloid and hypertrophic scars. Plast Reconstr Surg 119(3):844–851
8. Wiener TC (2008) Relationship of incision choice to capsular contracture. Aesthet Plast Surg 32(2):303–306
9. Younan GJ, Heit YI, Dastouri P, Kekhia H, Xing W, Gurish MF, Orgill DP (2011) Mast cells are required in the proliferation and remodeling phases of microdeformational wound therapy. Plast Reconstr Surg 128(6):649e–658e
10. Arad E, Navon-Venezia S, Gur E, Kuzmenko B, Glick R, Frenkiel-Krispin D, Kramer E, Carmeli Y, Barnea Y (2013) Novel rat model of methicillin-resistant *Staphylococcus aureus*-infected silicone breast implants: a study of biofilm pathogenesis. Plast Reconstr Surg 131(2):205–214
11. Jacombs A, Tahir S, Hu H, Deva AK, Almatroudi A, Wessels WLF, Bradshaw DA, Vickery K (2014) In vitro and in vivo investigation of the influence of implant surface on the formation of bacterial biofilm in mammary implants. Plast Reconstr Surg 133(4):471e–480e
12. Bergmann PA, Tamouridis G, Lohmeyer JA, Mauss KL, Becker B, Knobloch J, Mailänder P, Siemers F (2014) The effect of a bacterial contamination on the formation of capsular contracture with polyurethane breast implants in comparison with textured silicone implants—an animal study. J Plast Reconstr Aesthet Surg 67(10):1364–1370
13. Kyle DJT, Bayat A (2015) Enhanced contraction of a normal breast-derived fibroblast-populated three-dimensional collagen lattice via contracted capsule fibroblast-derived paracrine factors: functional significance in capsular contracture formation. Plast Reconstr Surg 135(5):1413–1429
14. Frame J, Kamel D, Olivan M, Cintra H (2015) The in vivo pericapsular tissue response to modern polyurethane breast implants. Aesthet Plast Surg 39(5):713–723
15. Silva EN, Ribas-Filho JM, Czeczko NG, Pachnicki JPA, Montemor Netto MR, Lipinski LC, Noronha L, Colman J, Zeni JO, Carvalho CA (2016) Histological evaluation of capsules formed by silicon implants coated with polyurethane foam and with a textured surface in rats. Acta Cir Bras 31(12):774–782
16. Segreto F, Carotti S, Tosi D, Pendolino AL, Marangi GF, Morini S, Persichetti P (2016) Toll-like receptor 4 expression in human breast implant capsules: localization and correlation with estrogen receptors. Plast Reconstr Surg 137(3):792–798
17. Danino MA, Nizard N, Paek LS, Govshievich A, Giot JP (2017) Do bacteria and biofilm play a role in double-capsule formation around macrotextured implants? Plast Reconstr Surg 140(5):878–883
18. Calobrace MB, Capizzi PJ (2014) The biology and evolution of cohesive gel and shaped implants. Plast Reconstr Surg 134(1S):6S–11S
19. Duxbury PJ, Harvey JR (2016) Systematic review of the effectiveness of polyurethane-coated compared with textured silicone implants in breast surgery. J Plast Reconstr Aesthet Surg 69(4):452–460
20. Adams WP, Culbertson EJ, Deva AK, Magnusson MR, Layt C, Jewell ML, Mallucci P, Héden P (2017) Macrotextured breast implants with defined steps to minize bacterial contamination around the device: experience in 42.000 implants. Plast Reconstr Surg 140(3):427–431
21. Barr S, Hill EW, Bayat A (2017) Functional biocompatibility testing of silicone breast implants and a novel classification system based on surface roughness. J Mech Behav Biomed Mater 75:75–81
22. Vieira JV, D'Acampora AJ, Marcos ABW, di Giunta G, Vasconcellos ZAA, Ely JB, Neves RE, Figueiredo CP (2010) Vascular endothelial growth factor overexpression positively modulates the characteristics of periprosthetic tissue of polyurethane-coated silicone breast implant in rats. Plast Reconstr Surg 126(6):1899–1910
23. Abramo AC, de Oliveira VR, Ledo-Silva MC, de Oliveira EL (2010) How texture-inducing contraction vectors affect the fibrous capsule shrinkage around breasts implants? Aesthet Plast Surg 34(5):555–560
24. Minami E, Koh IHJ, Ferreira JCR, Waitzberg AFL, Chifferi V, Rosewick TF, Pereira MD, Saldiva PHN, Figueiredo LFP (2006) The composition and behavior of capsules around smooth and textured breast implants in pigs. Plast Reconstr Surg 118(4):874–884
25. Balderrama CMSR, Ribas-Filho JM, Malafaia O, Czeczko NG, Dietz UA, Sakamoto DG, Bittencourt LPM (2009) Healing reaction to mammary prostheses covered by textured silicone and silicone foam in rats. Acta Cir Bras 24(5):367–376
26. Loch-Wilkinson A, Knight KJBRJW, Wessels WLF, Magnusson M, Papadopoulos T, Connell T, Lofts J, Locke M, Hopper I, Cooter R, Vickery K, Prince HM, Deva AK (2017) Breast implant-associated anaplastic large cell lymphoma in Australia and New Zealand: high-surface-area textured implants are associated with increased risk. Plast. Reconstr. Surg. 140(4):645–654
27. Foley TT, Saggers GC, Moyer KE, Ehrlich HP (2011) Rat mast cells enhance fibroblast proliferation and fibroblast-populated collagen lattice contraction trough gap junctional intercellular communications. Plast Reconstr Surg 127(4):1478–1486
28. Foley TT, Ehrlich HP (2013) Through gap junction communications, co-cultured mast cells and fibroblasts generate fibroblasts activities allied with hypertrophic scarring. Plast Reconstr Surg 133(5):1036–1044
29. Foley TT, Ehrlich HP (2014) Mast cells prevent dexamethasone-induced cell death of cultured fibroblasts: relationship to gap junctional intercellular communications. Plast Reconstr Surg 133(5):638e–644e
30. Brazin J, Malliaris S, Groh B, Mehrara B, Hidalgo D, Otterburn D, Silver RB, Spector JA (2014) Mast cells in the periprosthetic breast capsule. Aesthet Plast Surg 38(3):592–601
31. Isenberg JS (2014) Time spent before the mast: an emerging role for mast cells in prosthetic breast implant capsule formation. Aesthet Plast Surg 38(4):815–816
32. Bresnick SD (2017) Prophylactic leukotriene inhibitor therapy for the reduction of capsular contracture in primary silicone breast augmentation: experience with over 1100 cases. Plast Reconstr Surg 139(2):379e–385e
33. Chen H, Xu Y, Yang G, Zhang Q, Huang X, Yu L, Dong X (2017) Mast cell chymase promotes hypertrophic scar fibroblast proliferation and collagen synthesis by activating TGF-β1/ Smads signaling pathway. Exp Ther Med 14(5):4438–4442
34. Moreira M, Fagundes DJ, Simões MJ, Oliveira MCBM, Previdelli ITS, Moreira AC (2009) Zafirlukast pocket delivery impairs the capsule healing around textured implants in rats. Aesthet Plast Surg 33(1):90–97
35. Pistorio AL, Ehrlich HP (2011) Modulatory effects of connexin-43 expression on gap junction intercellular communications with mast cells and fibroblasts. J Cell Biochem 112(5):1441–1449

36. Prantl L, Schreml S, Fichtner-Feigl S, Pöppl N, Eisenmann-Klein M, Schwarze H, Füchtmeier B (2007) Clinical and morphological conditions in capsular contracture formed around silicone breast implants. Plast Reconstr Surg 120(1):275–284
37. Graf R, Ascenço ASK, Freitas R, Balbinot P, Peressutti C, Costa DFB, Santos FHCR, Ratti MAS, Kulchetscki RM (2015) Prevention of capsular contracture using leukotriene antagonists. Plast Reconstr Surg 136(5):592e–596e
38. Ceua-Fiocruz (2008) Manual de Utilização de Animais/FIOCRUZ. 1ª Ed. Ministério da Saúde, Rio de Janeiro: FIOCRUZ
39. Avninder S, Ylaya K, Hewitt SM (2008) Tissue microarray: a simple technology that has revolutionized research in pathology. J Postgrad Med 54(2):158–162
40. Zwieten A (2013) Tissue microarray technology and findings for diagnostic immunohistochemistry. Pathology 45(1):71–79
41. Lee SG, Lee SD, Kim MK, Ryu WS, Jung SP, Kim S, Kim HY, Yoon ES, Kim CH, Nam SJ, Bae JW (2015) Effect of antiadhesion barrier solution and fibrin on capsular formation after silicone implant insertion in a white rat model. Aesthet Plast Surg 39(1):162–170
42. Unlu RE, Yilmaz AD, Orbay H, Can B, Tekdemir I, Sensoz O (2007) Influence of rifampin on capsule formation around silicone implants in a rat model. Aesthet Plast Surg 31(4):358–364
43. Bastos EM, Neto MS, Garcia EB, Veiga DF, Han YA, Denadai R, Santos RA, Ferreira LM (2007) Effect of zafirlukast on capsular contracture around silicone implants in rats. Aesthet Plast Surg 31(5):559–565
44. Vieira JV, D'Acampora A, Neves FS, Mendes PR, Vasconcellos ZAA, Ely JB, Neves RE, Figueiredo CP (2016) Capsular contracture in silicone breast implants: insights from rat models. An Acad Bras Cienc 88(3):1459–1470
45. Boyko TV, Longaker MT, Yang GP (2017) Laboratory models for the study of normal and pathologic wound healing. Plast Reconstr Surg 139(3):654–662
46. Wagenführ Júnior J (2007) Comparative histopathological analysis of coverings from silicone and polyurethane foams implanted in mice. ReSoc Bras Cir Plast 22(1):19–23
47. Haddad Filho D, Zveibel DK, Alonso N, Gemperli R (2007) Comparison between textured silicone implants and those bonded with expanded polytetrafluoroethylene in rats. Acta Cir Bras 22(3):187–194
48. Gancedo M, Ruiz-Corro L, Salazar-Montes A, Rincón AR, Armendáriz-Borunda J (2008) Pirfenidone prevents capsular contracture after mammary implantation. Aesthet Plast Surg 32(1):32–40
49. Wagenführ Júnior J, Ribas-Filho JM, Nascimento MM, Ribas FM, Wanka MV, Godoi AL (2012) Histopathological reaction over prosthesis surface covered with silicone and polyurethane foam implanted in rats. Acta Cir Bras 27(12):866–873
50. Bui JM, Perry TA, Ren CD, Nofrey B, Teitelbaum S, Epps DE (2015) Histological characterization of human breast implant capsules. Aesthet Plast Surg 39(3):306–315
51. Thevenot T, Baker DW, Weng H, Sun M, Tang L (2011) The pivotal role of fibrocytes and mast cells in mediating fibrotic reactions to biomaterials. Biomaterials 32(33):8394–8403
52. Hwang K, Sim HB, Huan F, Kim DJ (2010) Myofibroblasts and capsular tissue tension in breast capsular contracture. Aesthet Plast Surg 34(6):716–721
53. Rocha-De-souza CM, Berent-Maoz B, Mankuta D, Moses AE, Levi-Schaffer F (2008) Human mast cell activation by *Staphylococcus aureus*: interleukin-8 and tumor necrosis factor alpha release and the role of toll-like receptor 2 and CD48 molecules. Infect Immun 76(10):4489–4497